FULL PAPER

Design Principle of Conjugated Polyelectrolytes to Make Them Water-Soluble and Highly Emissive

Kangwon Lee, Hyong-Jun Kim, and Jinsang Kim*

The correlation between the molecular design of a conjugated polyelectrolyte (CPE) and its aggregated structure and the emissive properties in water is systematically investigated by means of UV–vis spectrometry, fluorescence spectroscopy, and scanning/transmission electron microscopy. Five different and rationally designed CPEs having carboxylic acid side chains are synthesized. All five conjugated polyelectrolytes are seemingly completely soluble in water in visual observation. However, their quantum yields are dramatically different, changing from 0.45 to 51.4%. Morphological analysis by electron microscopy combined with fluorescence spectrophotometry reveals that the CPEs form self-assembled aggregates at the nanoscale depending on the nature of their side chains. The feature of the self-assembled aggregates directly determines the emissive property of the CPEs. The nature and the length of the spacer between the carboxylic acid group and the CPE backbone have a strong influence on the quantum yield of the CPEs. Our study demonstrates that bulky and hydrophilic side chains and spacers are required to achieve complete water-solubility and high quantum yield of CPEs in water, providing an important molecular design principle to develop functional CPEs.

1. Introduction

A conjugated polyelectrolyte (CPE)[1,2] a conjugated polymer containing a charged (anionic or cationic) group, has received considerable attention for its bio-applications such as solution-based DNA sensor,[3–11] DNA microarray,[12–14] protein sensor,[15–24] bioimaging[25–28] as well as optoelectronic applications such as organic semiconductors,[29–31] light-emitting devices,[32,33] and actuators.[34] The ionic side group plays an important role to provide CPEs with water-solubility that is central to many

biological applications. In addition, maintaining the emissive property of a CPE in aqueous solution is another requirement for many biosensor applications because the merit of using conjugated polymers as a sensor is their amplified fluorescence signaling property upon environmental changes.[35–45]

However, in this regard, CPE inherently has a critical solubility limitation in aqueous environment because the π-conjugated polymer backbone is chemically hydrophobic and structurally rigid. The rigid-rod and hydrophobic nature of CPEs induces polymer aggregation via intermolecular hydrophobic interaction among the polymer backbones in aqueous environment.[37,38,46] Therefore, the solubility of CPE in water is significantly low, consequently inducing significant decrease in the fluorescence quantum yield due to the aggregation-induced self-quenching.[47–51]

Moreover, once CPEs are completely dried, it is tremendously difficult to re-dissolve them in water due to the rigid hydrophobic nature of the backbone and resulting strong and cohesive aggregation. Besides the solubility issue, there is another requirement for CPE to be useful for biological applications. To achieve efficient and convenient bio-conjugation between the CPE and a biological molecule, CPEs should have an efficient and convenient functional group such as a carboxylic acid group or an amine group.[52,53] Due to these demanding requirements, it remains a difficult task to develop highly emissive and completely water-soluble functional CPEs.

Several research groups have developed CPE-based functional systems by utilizing the emissive property of CPEs. Leclerc et al. developed DNA sensors using cationically charged polythiophene derivatives. Charge–charge interaction between the cationic CPE and a single strand DNA and subsequent detection of the complementary DNA produces a conformation change of the CPE and consequent color change as a sensory signal.[7,15,54–57] Bazan and co-workers have reported signal amplifying biosensors based on cationically charged CPEs and fluorescence resonance energy transfer (FRET).[4] Schanze et al. investigated CPE systems and reported amplified fluorescence quenching of sulfonated CPEs due to π–π aggregation of the rigid linear CPEs in aqueous media.[37,38,40] Bunz and co-workers have investigated pH-dependent optical properties of CPEs by modulating carboxylic acid side-chain.[58] Furthermore, cationic gold nanoparticles conjugated with carboxylated CPEs

Dr. K. Lee,[+] Dr. H.-J. Kim,[++] Prof. J. Kim
Department of Materials Science and Engineering
University of Michigan
Ann Arbor, MI 48109, USA
E-mail: jinsang@umich.edu
Prof. J. Kim
Department of Chemical Engineering
Macromolecular Science and Engineering
Biomedical Engineering
University of Michigan
Ann Arbor, MI 48109, USA
[+] Present address: School of Engineering and Applied Science, Harvard University, MA, USA
[++] Present address: College of Engineering, Kongju National University

www.MaterialsViews.com

ADVANCED
FUNCTIONAL
MATERIALS
www.afm-journal.de

FULL PAPER

polyelectrolytes have successfully been developed for bacteria identification vehicles.[59] Recently, completely water-soluble CPEs have been also reported.[53,60] Understanding the correlation among the quenching dynamics, the chemical structure of receptor-functionalized CPEs, and the fluorescence efficiency is critically important to develop biosensory materials based on water-soluble CPEs. However, to our knowledge there has not been any article that comprehensively and systematically provides design principles to develop highly emissive and completely water-soluble CPEs.

We have rationally designed and prepared a series of PPE-based CPEs and systematically investigated the effects of the side chain structure on the solubility and the fluorescence quantum yield of the CPEs in aqueous environment. Here, we report our comprehensive quantum yield study, scanning transmission electron microscopy and conventional/cryogenic transmission electron microscopy (TEM) study to reveal the correlation among the chemical and structural characteristics of the side chain of the CPEs, their molecular assembly, and their emissive property. We chose carboxylic acid moiety for this study as a pendant ionic group considering that it is the most convenient functional group for bioconjugation with the ubiquitous amine group present in biological molecules. As the molecular design parameter, we controlled the bulkiness of the side chain, the length of the linker molecule between the conjugated backbone and the carboxylic acid group, and the hydrophobic and hydrophilic property of the linker as illustrated in **Figure 1**.

2. Results and Discussion

2.1. Synthesis of the Monomers and Polymers (P1-P5)

Synthesis of Bis(2-ethylhexyl) 2,5-diiodoterephthalate (M1): 2,5-diiodoterephthalic acid (**1**, 0.3 g, 0.72 mmol), 2-ethyl-1-hexanol (0.28 g, 2.16 mmol), toluene (20 mL), and 0.1 mL of concentrated H_2SO_4 were heated for 24 h to reflux, with separation of the water using a Dean–Stark trap. Reaction mixture was cooled down and the organic layer was washed with water and dried with $MgSO_4$. Further purification was done by column chromatography (ethyl acetate: hexane = 1:15 v/v) to get viscous yellow oil (0.14 g, 30%). ^{1}H-NMR (500 MHz, CDCl$_3$): δ/ppm 8.26 (s, 2H, aromatic), 4.27 (d, 4 H, -OCH$_2$-), 1.79 (m, 2H, -CH-), 1.55-1.30 (m, 16H, -CH$_2$-), 0.95 (m, 12H, CH$_3$). ^{13}C-NMR (125 MHz, CDCl$_3$): δ/ppm 165.5, 139.9, 138.1, 92.7, 68.6, 38.9, 30.6, 29.0, 24.0, 23.0, 14.1, 11.1. HRMS (Voltage EI+): calculated m/z of [M+] 642.0691; measured m/z 642.0679.

Diethyl 4,4′-(2,5-diiodo-1,4-phenylene)bis(oxy)dibutanoate (M2): To a solution of 2,5-diiodo-1,4-hydroquinone (**2**, 1.0 g, 2.76 mmol) were added a potassium carbonate (1.615 g, 8.28 mmol), ethyl 4-bromobutyrate (1.615 g, 8.28 mmol) and DMF (15 mL) and reaction mixture was stirred at 80 °C for 48 h. After the reaction, reaction mixture was cooled down and filtered. DMF was removed with rotary evaporator at reduced pressure. Crude mixture was re-dissolved in chloroform and extracted twice with deionized water. After drying over $MgSO_4$ and filtering, chloroform was removed in vacuo. Further purification was done by column chromatography (ethyl acetate: hexane = 1:1 v/v) and the following recrystallization in methanol at –18 °C to give white waxy powder (yield: 0.65 g, 41%). ^{1}H-NMR (500 MHz, CDCl$_3$): δ/ppm 7.10 (s, 2H, aromatic), 4.20 (m, 4H, -OCH$_2$CH$_3$), 4.01 (t, 4H, -OCH$_2$-), 2.60 (t, 4H, -CH$_2$COO-), 2.15 (m, 4H, -CH$_2$-), 1.27 (t, 6H, -CH$_3$). ^{13}C-NMR (125 MHz, CDCl$_3$): δ/ppm 173.1, 152.7, 122.5, 86.1, 69.9, 60.3, 30.6, 24.4, 14.1. Elemental analysis calcd; C 36.63, H: 4.10, obsd; C: 36.71, H: 4.15.

Diethyl 7,7′-(2,5-diiodo-1,4-phenylene)bis(oxy)diheptanoate (M3): Synthetic procedure for this compound is the same as that for **M2** except for using ethyl 7-bromoheptanoate (2 g, 8.43 mmol) as a reactant and different column eluent (ethyl acetate: hexane = 1:4 v/v) for column purification (yield: 0.89 g, 47%). ^{1}H-NMR (500 MHz, CDCl$_3$): δ/ppm 7.18 (s, 2H, aromatic C-H), 4.15 (m, 4H, COO-CH$_2$-CH$_3$), 3.94 (t, 4H, O-CH$_2$-), 2.33
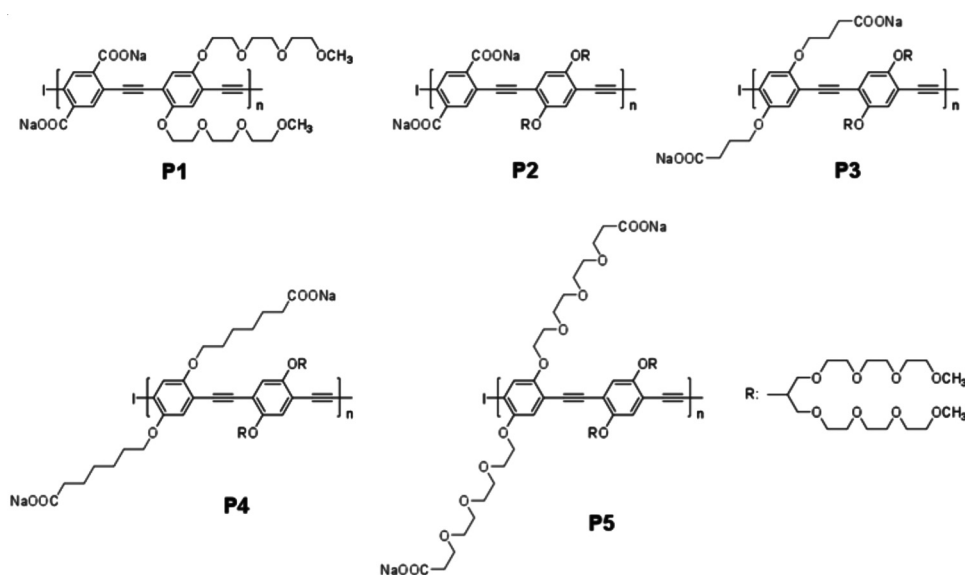
Figure 1. The chemical structure of the CPEs (**P1-P5**).

FULL PAPER

(t, 4H, CH$_2$-CH$_2$-CO-), 1.82 (m, 4H, -CH$_2$-), 1.69 (m, 4H, -CH$_2$-), 1.54 (m, 4H, -CH$_2$-), 1.42 (m, 4H, -CH$_2$-), 1.27 (t, 6H, -CH$_3$). ^{13}C-NMR (125 MHz, CDCl$_3$): δ/ppm 173.1, 152.7, 122.5, 86.1, 70.1, 60.3, 33.5, 31.3, 29.1, 25.7, 25.5, 14.1. Elemental analysis calcd; C 42.75, H: 5.38, obsd; C: 42.85, H: 5.40.

Tert-butyl 3-(2-(2-(2-hydroxyethoxy)ethoxy)ethoxy)propanoate (**3**): This compound was prepared by procedure in a previous literature through a slight modification.[52] In 1000 mL of 2-necked round-bottomed flask, triethylene glycol (128 mL, 0.40 mol) is dissolved in 500 mL of THF. 0.34 g (14.8 mmol) of sodium lump was sliced and added to the solution under argon purging. The solution was vigorously stirred to dissolve sodium completely. After no more gas or bubble, *tert*-butyl acrylate (48 mL, 0.33 mol) was added to the solution. The reaction solution was stirred under argon atmosphere at room temperature for 20 h. The solution was neutralized with 1 M HCl and THF was evaporated at reduced pressure. Crude compound was suspended to saturated brine and extracted with ethyl acetate. Organic layer was washed with saturated NaCl solution and water again and dried over anhydrous MgSO$_4$ (yield: 58.5 g, 53%). ^{1}H-NMR (500 MHz, CDCl$_3$): δ/ppm 3.75-3.21 (m, 14H, -OCH$_2$-), 2.69 (broad s, 1H, OH), 2.51 (t, 2H, -CH$_2$COO-), 1.45 (s, 9H, -C(CH$_3$)$_3$). ^{13}C-NMR (125 MHz, CDCl3): δ/ppm 28.2, 36.3, 61.7, 66.9, 70.4, 70.5, 70.6, 70.7, 80.6, 171.0.

Tert-butyl3-(2-(2-(2-(toluenesulfonyloxy)ethoxy)ethoxy)ethoxy)-propanoate (**4**): Compound **3** (58.5 g, 0.21 mol) and triethylamine (171 mL) was dissolved in anhydrous dichloromethane (290 mL) and the solution was cooled down to 4 °C using iced bath. *p*-toluenesulfonyl chloride (46.82 g, 0.245 mol) in 100 mL of dichloromethane was added dropwise. The temperature of reaction solution was slowly increased to room temperature and the solution was stirred overnight. After the reaction, the solution was poured into 1300 mL of 1 M HCl and the aqueous phase is removed. Organic phase was washed with saturated NaCl solution and dried over MgSO$_4$. The compound was purified by column chromatography (ethyl acetate: hexane = 1: 1 v/v) (yield: 69.9 g, 77%). ^{1}H-NMR (500 MHz, CDCl$_3$): δ/ppm 7.60 (d, J = 5 Hz, 2H, aromatic H), 7.18 (d, J = 5 Hz, 2H, aromatic H), 3.97 (t, 2H, S-O-CH$_2$), 3.58-3.31 (m, 12H, -O-CH$_2$-), 2.29 (t, 2H, -CH$_2$-COO), 2.25 (s, 3H, Ar-CH$_3$), 1.25 (s, 9H, C(CH$_3$)$_3$). ^{13}C-NMR (125 MHz, CDCl$_3$): δ/ppm 21.8, 28.2, 36.4, 67.0, 68.8, 69.4, 70.5, 70.6, 70.7, 70.8, 80.6, 128.1, 130.0, 133.1, 144.9, 171.0. HRMS (C$_{20}$H$_{32}$O$_8$S+Na): calculated m/z of [M+Na] 455.1705; measured m/z 455.1714.

1,4-diiodo-2,5-bis(11-(*tert*-butoxycarbonyl)-3,6,9-trioxaundecyloxy)benzene (**5**): Compound **4** (11.28 g, 26.08 mmol), compound **2** (3.93 g, 10.87 mmol), potassium iodide (0.018 g, 0.11 mmol), potassium carbonate (9 g, 65.22 mmol) and 30 mL of 2-butanone were added to a 250 mL of two neck round-bottomed flask with condenser. Reaction solution was refluxed for 38 h and 2-butanone was evaporated at reduced pressure. The crude mixture was suspended to methylene chloride and washed with 1 M HCl. The organic layer was again washed with saturated NaCl and dried over MgSO$_4$. Further purification was achieved by column chromatography on silica gel (ethyl acetate: hexanes = 7:3 v/v). Compound was again chromatographed on silica gel (ethyl acetate: hexanes = 1:1 v/v) (yield: 4.26 g, 44%). ^{1}H-NMR (500 MHz, CDCl$_3$): δ/ppm 7.22 (s, 2H, aromatic), 4.15 (t, 4H, -OCH$_2$-), 3.87 (t, 4H, -OCH$_2$-), 3.8-3.6 (m, 20H, -OCH$_2$-),

2.51 (t, 4H, -CH$_2$COO-), 1.42 (s, 18H, -C(CH$_3$)$_3$), ^{13}C-NMR (125 MHz, CDCl$_3$): δ/ppm 28.3, 36.4, 67.1, 69.8, 70.4, 70.6, 70.7, 70.8, 80.7, 86.6, 123.6, 153.3, 171.1. HRMS (C$_{32}$H$_{52}$I$_2$O$_{12}$+Na): calculated m/z of 905.1435; measured m/z 905.1442.

1,4-diiodo-2,5-bis(11-carboxy-3,6,9-trioxaundecyloxy)benzene (**M4**): To a 4.00 g (4.53 mmol) of compound 5 was added 85 mL of trifluoroacetic acid (CF$_3$COOH). As soon as trifluoroacetic acid was added, the color of reaction mixture turned red. The mixture was stirred at room temperature for overnight. The reaction mixture was evaporated at reduced pressure. The crude mixture was dissolved in chloroform and washed with water three times. Organic layer was dried over MgSO$_4$ and filtered. The filtrate was evaporated to dryness and the compound **M4** was further dried in vacuo and solidified to white-yellow waxy powder (yield: 2.57 g, 74%). ^{1}H-NMR (500 MHz, CDCl$_3$): δ/ppm 9.8 (broad s, 2H, -COOH), 7.22 (s, 2H, aromatic), 4.15 (t, 4H, -OCH$_2$-), 3.83 (t. 4H, -OCH$_2$-), 3.81-3.50 (m, 20H, -OCH$_2$-), 2.60 (t, 4H, -CH$_2$COOH). ^{13}C-NMR (125 MHz, CDCl$_3$): δ/ppm 35.2, 66.7, 69.8, 70.5, 70.7, 70.8, 70.9, 71.32, 86.6, 123.6, 153.3, 175.4. MS (Voltage ESI-): calculated m/z of [M-H] 769.0218; measured m/z 769.0221.

Polymer synthesis P1: **M1** (65 mg, 0.14 mmol) and **M5** (90 mg, 0.14 mmol) were placed into a Schlenck flask (50 mL). Toluene (1.5 mL) and diisopropylamine (3 mL) were added. After complete dissolution of two monomers, the solution was degassed by three times of vacuum and argon purging. In a separate Schlenck flask, tetrakistriphenylphosphine palladium (0) and copper (I) iodide were dissolved in toluene (1.5 mL) under a nitrogen atmosphere in a glove box and degassed. The degassed solution containing catalyst was cannulated onto the monomer solution. After transfer of the catalysis solution to monomer solution, polymerization solution was finally degassed again and allowed to stir under argon purging at 55 °C for 2 days. The reaction mixture filtered with 0.45 micrometer membrane syringe. The toluene solution was precipitated in methanol 2 times. For deprotection of ethylhexyl group of carboxylic group, the collected fluorescent yellow precipitate was redissolved in 100 mL of tetrahydrofuran (THF) and 1 M of NaOH (100 mL) was added. The solution was stirred overnight at 35 °C. THF was evaporated at the reduced pressure, filtered and the water solution was dialyzed against deionized water for 3 days (membrane MW cut off: 12 000–14 000 gmol^{-1}, 10 × 4 L water exchanges). The polymer solution was lyophilized to yield a yellow solid (74 mg, 80%). ^{1}H-NMR (500 MHz, D$_2$O): δ/ppm 7.60 (s, 2H, aromatic), 7.11 (s, 2H, aromatic), 4.13 (broad t, 4H, -OCH$_2$-), 3.90-3.30 (broad m, 2OH, -OCH$_2$CH$_2$-), 3.15 (s, 6H, -OCH$_3$), Molecular weight based on PS-GPC in THF before hydrolysis of ethylhexylgroup M_n = 163 700, M_w = 624 600, PDI = 3.82.

P2: Except **M6** (85 mg, 95.4 μmol) instead of **M5**, the polymerization step was followed by synthetic route of **P1** above. After polymerization, polymer solution was centrifuged to get the supernatant (3500 rpm). The supernatant solution was evaporated and redissolved in 10 mL tetrahydrofuran and 10 mL of 1 M NaOH solution. The solution was stirred overnight at 35 °C and evaporated at reduced pressure. The solution was dissolved in deionized water and centrifuged to remove the impurity insoluble to water. The water solution was dialyzed against deionized water for 3 days. Centrifugation was again

Materials
Views
www.MaterialsViews.com

ADVANCED
FUNCTIONAL
MATERIALS
www.afm-journal.de

FULL PAPER

conducted to get supernatant after dialysis. The polymer solution was lyophilized to yield a yellow solid (91 mg, 87%). ^{1}H-NMR (500 MHz, D$_2$O): δ/ppm 7.58 (s, 2H, aromatic), 7.12 (s, 2H, aromatic), 4.13 (m, 2H, -OCH-), 3.80-3.20 (broad m, 56H, -OCH$_2$-), 3.11 (s, 12H, -OCH$_3$). GPC-based molecular weight before the cleavage of protection group, M_n = 32,100 gmol^{-1}, M_w = 105,900 gmol^{-1}, PDI = 3.3.

P3: A general procedure about polymerization is identical to the method for **P1**. Monomer **M2** (40.8 mg, 69.1 μmol), monomer **M6** (61.6 mg, 69.1 μmol), toluene (1.0 mL), and diisopropylamine (2 mL) are placed into a 50 mL of Schlenck flask. After complete dissolution of two monomers, the solution was degassed by three times of vacuum and argon purging. In a separate Schlenck flask, tetrakistriphenylphosphine palladium (0) (5 mol% of the monomer) and copper (I) iodide (5 mol% of the monomer) were transferred under a nitrogen atmosphere of a glove box and argon was purged in the Schlenck flask for 10 min. Two catalysts were dissolved in toluene (1.0 mL) and degassed by three times of vacuum and argon purging. The degassed solution containing catalyst was cannulated onto monomer solution. After transfer of the catalyst solution to monomer solution, three cycles of degassing to a polymer solution was finally done again. The polymer solution was allowed to stir under argon purging at 55 °C for 2 days. The reaction mixture was filtered with 0.45 micrometer membrane syringe. The mixture solution was concentrated at reduced pressure and precipitated in diethylether (15 mL). The crude polymer was redissolved in 15 mL of dioxane and the solution was mixed with 10% aqueous NaOH solution (15 mL). Solution was stirred under argon atmosphere at room temperature for 12 h. Polymer solution was centrifuged and dialyzed against deionized water for 2 days (10 × 4 L water exchanges). The polymer solution was lyophilized to yield a yellow solid (51 mg, 60%). ^{1}H-NMR (500 MHz, D$_2$O): δ/ppm 7.27 (s, 2H, aromatic), 7.15 (s, 2H, aromatic), 4.03 (broad m, 6H, -CH$_2$CH$_2$O-, -OCH-), 3.81-3.21 (broad m, 56H, -OCH$_2$CH$_2$), 3.18 (broad s, 12H, -OCH$_3$), 2.25 (broad t, 4H, -CH$_2$CH$_2$COO-), 1.87 (broad m, 4H, -CH$_2$CH$_2$CH$_2$-), GPC (THF) based M_n = 73,100 gmol^{-1}, M_w = 214,200 gmol^{-1}, PDI = 2.93.

P4: Except **M3** (41.85 mg, 62 μmol) instead of **M2**, the polymerization step was conducted by synthetic route of **P3** above. After the polymerization, polymer mixture was centrifuged to get the supernatant (3500 rpm). The supernatant solution was concentrated at reduced pressure, precipitated in ether, and washed with acetone. The polymer was redissolved in 10 mL tetrahydrofuran and 10 mL of 1 M sodium hydroxide solution. The solution was stirred overnight at 35 °C and evaporated at reduced pressure. The solution was dissolved in DI water and centrifuged to remove the unknown impurity. The water solution was dialyzed against deionized water for 3 days. During the dialysis, fibril type aggregations observed due to the hydrophobic long alkyl chain and the protonation of carboxylic group. The polymer solution was lyophilized to yield a yellow solid (46 mg, 57%). A solid **P4**, of which a carboxylic group is protonated, was completely soluble in water (pH = 8). ^{1}H-NMR (500 MHz, D$_2$O): δ/ppm 7.01 (s, 2H, aromatic), 6.75 (s, 2H, aromatic), 4.41 (m, 2H, -OCH-), 3.95 (t, 4H, -OCH$_2$-), 3.80-3.23 (broad m, 56H, -OCH$_2$-), 3.15 (s, 12H, -OCH$_3$), 2.05 (t, 4H, -CH$_2$COO-), 1.78-1.10 (broad m, 16H, -CH$_2$-), GPC (THF) based M_n = 19 200 gmol^{-1}, M_w = 57 800 gmol^{-1}, PDI = 3.01.

P5: **M4** (60.6 mg, 78.7 μmol) and **M6** (73.6 mg, 82.6 μmol) were placed into a 50 mL of Schlenck flask and DMF (2 mL) and diisopropylamine (1 mL) were added to the reaction vessel. After complete dissolution of two monomers, the solution was degassed by three times of vacuum and argon purging. In a separate Schlenck flask, tetrakistriphenylphosphine palladium(0) (1 mol% of the monomer) and copper(I) iodide (1 mol% of the monomer) were transferred under a nitrogen atmosphere of a glove box and argon was purged in the Schlenck flask for 10 min. Two catalysts were dissolved in morpholine (1 mL) and degassed by three times of vacuum and argon purging. The degassed solution containing catalyst was cannulated onto monomer solution. After transfer of the catalyst solution to monomer solution, three cycles of degassing to a polymer solution was finally done again. The polymer solution was allowed to stir under argon purging at 55 °C for 2 days. The solvent was evaporated to dryness. The crude polymer was redissolved in 50 mL of 1 M sodium hydroxide solution and stirred under argon atmosphere at room temperature for 1 h. Polymer solution was centrifuged and the supernatant was dialyzed against deionized water for 2 days (10 × 4 L water exchanges). The polymer solution was lyophilized to yield a yellow waxy solid (77 mg, 67%). ^{1}H-NMR (500 MHz, D$_2$O): δ/ppm 8.30 (broad s, 2H, -COOH), 7.25 (s, 2H, aromatic), 7.09 (s, 2H, aromatic), 4.16 (t, 4H, -OCH$_2$-), 4.08 (m, 2H, -OCH-), 3.8-3.2 (broad m, 80H, -OCH$_2$CH$_2$O-), 3.15 (s, 12H, -OCH$_3$), 2.27 (s, 4H, -CH$_2$COO-), molecular weight; M_n by ^{1}H-NMR end analysis = 14 200.

P5-A: End-capping reaction was conducted in-situ after polymerization of **P5** was finished. 4-ethynylbenzoic acid (11 mg, 79 μmol) as an end-capper was dissolved in DMF (0.5 mL) and DIPA (0.2 mL). End-capper solution was degassed and cannulated onto polymer solution. A trace amount of palladium catalyst and cupper iodide in DMF (0.5 mL) degassed by vacuum and argon purging recycles was also added to polymer solutions. The polymer solution was allowed to stir under argon purging at 55 °C for an additional 24 h. After the reaction, a work-up procedure for polymer recovery was same as **P5**. Two new peaks at ^{1}H-NMR analysis emerged at 7.78, 7.51 ppm corresponding to the aromatic protons of the end-capper, confirming that the carboxylic group was chemically attached.

2.2. Discussion for Synthesis of Monomers and Polymers

Synthetic routes for the preparation of all monomers and CPEs are described in **Schemes 1** and **2**. All polymers were prepared by the palladium-catalyzed Sonogashira-Hagihara copolymerization method. At first, we tried polymerization with a diiodophenyl unit having unprotected free carboxylic acid. However, reactions were not successful because the carboxylic group in the ortho-position caused a side reaction during the polymerization and resulted in a low molecular weight.[61–63] **P1** and **P2** were prepared by the copolymerization of a diiodophenyl monomer having carboxylic groups protected with ethylhexyl side chains. After the polymerization, the ethylhexyl group was hydrolyzed by base treatment to give a negatively charged carboxylate ion as a side chain to the polymer structure. A flexible
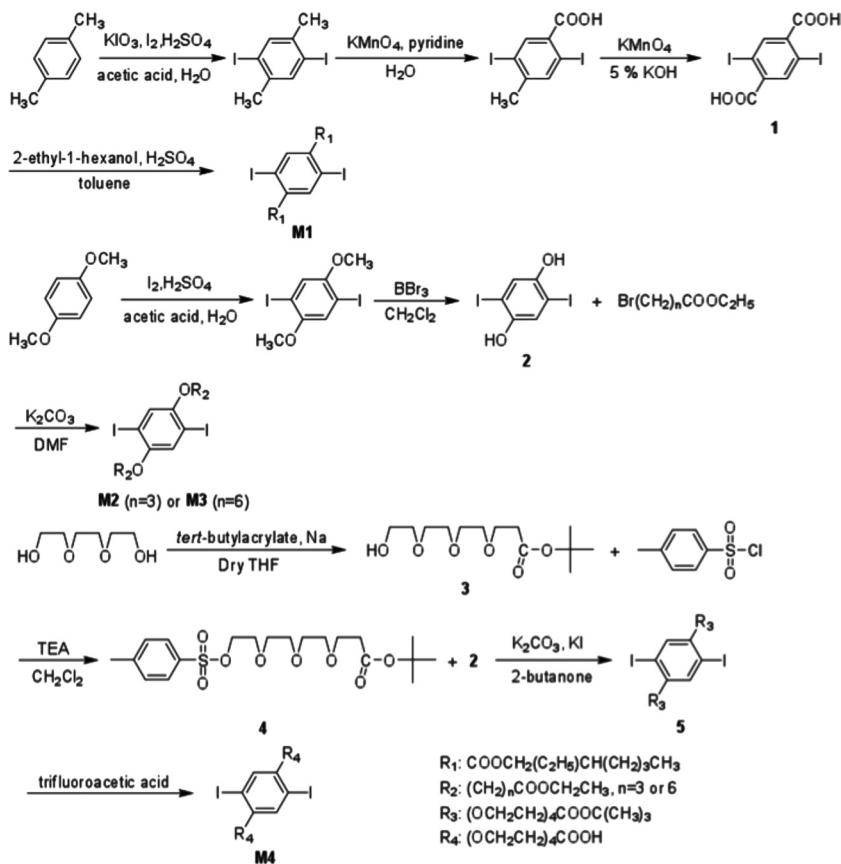
Scheme 1. Synthesis of Monomers **M1** to **M4**.

and hydrophilic ethylene oxide unit was also introduced in order to give good water solubility to the hydrophobic polymer backbone by suppressing the hydrophobic aggregation. **P3** and **P4** were also prepared by the polymerization of a diiodo monomer having ethyl-protected carboxylic groups to avoid the solubility problem of the free carboxylic acid group in organic solvents. Representative physical and photophysical data of the CPEs described in this contribution are summarized in **Table 1**. All CPEs were dissolved in water and showed blue-green emission having the emission λ_{max} of about 460 nm.

2.3. P1: Conventional CPE Design with Ionic and Non-Ionic Water-Soluble Side Chains

P1 is designed to have alternating ionic and non-ionic water-soluble side chains. This molecular design strategy has been conventionally used to make water-soluble CPEs in the literature. The precursor polymer of **P1** before the deprotection of the carboxylic acid group showed a well-defined 0–0 emission band at 487 nm and the quantum yield of 45% in chloroform (**Figure 2**). However, emission of **P1** in water after the deprotection

showed a blue-shifted and much weaker emission. Cleavage of the protecting group from the carboxlic moiety (electron-withdrawing group) will affect overall dipole moment and charge density of the polymer backbone (electron-donating group). The solvent polarity also should play a role in the blue shift.

The quantum yield of **P1** was only 0.45% in water. The solubility of **P1** in water was high enough to dissolve more than 1 mg of **P1** in 1 mL of deionized water. **P1** solution in water looked yellow and transparent in visual observation. However, even though the aqueous solution of **P1** looked to be transparent to the naked eye, our co-solvent study and surfactant study strongly imply that **P1** was aggregated in water. We examined the photoluminescence properties of **P1** in the water/methanol co-solvent system. As shown in **Figure 3**, the emission intensity of **P1** increased as the volume fraction of methanol was increased in the water/methanol mixture because methanol is a better solvent than water, suggesting **P1** aggregation in water. To further investigate the aggregation feature we conducted a surfactant study by using sodium dodecylsulfate (SDS, anionic), Tween20 (nonionic), and dodecyltrimethylammonium bromide (DTAB, cationic) and investigated their de-aggregation capability for **P1** in water (**Figure 4**).[64–68] Fluorescence emission intensity of **P1** was enhanced as the surfactant concentration was increased in all three cases likely due to de-aggregation of the polymer aggregates induced by the surfactants. The difference in the emission enhancement of **P1** at a given concentration of each surfactant indicates that the cationic surfactant DTAB most
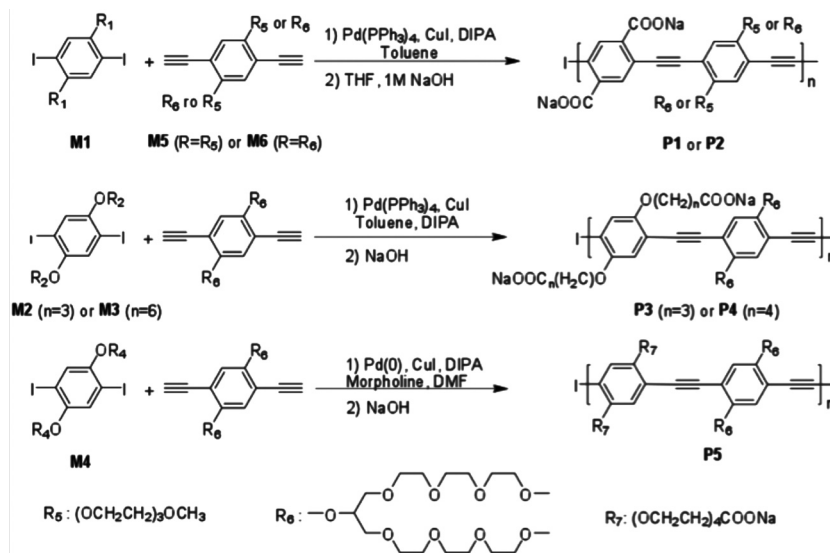
Scheme 2. Polymer synthesis (**P1–P5**).

www.MaterialsViews.com

ADVANCED
FUNCTIONAL
MATERIALS
www.afm-journal.de

FULL PAPER

Table 1. Physical properties of all polymers used in this study.

poly	M_n/gmol$^{-1a)}$	DP$^{b)}$	$\lambda_{max,abs}$/nm $\lambda_{max,em}$/nm	Stokes shift cm$^{-1c)}$	E_g/eV$^{d)}$	Φ_F (%, D$_2$O)$^{e)}$
P1	163,700	194	384	4110	2.14	0.45 ± 0.49
			456			
P2	32,100	29	368	5430	2.18	0.09 ± 0.02
			460			
P3	73,100	59	421	2150	2.54	31.6 ± 5.50
			463			
P4	19,200	15	406	3080	2.52	5.3 ± 0.55
			464			
P5 (or **P5-A**)	14,200	10	412	2390	2.64	51.4 ± 9.55 (36.6 ± 4.37)
			457			

$^{a)}$Molecular weight of all polymers except **P5** was measured by GPC before hydrolysis of the ethylhexyl protection. M_n for **P5** was done by ^{1}H-NMR end analysis in D$_2$O; $^{b)}$Degree of polymerization (DP) was calculated from the M_n and the molar mass of the repeat unit; $^{c)}$The magnitude of the Stokes shift was calculated by $\Delta = \lambda_{max,em} - \lambda_{max,abs}$; $^{d)}$The optical HOMO-LUMO energy gap is based on the low-energy onset in the solution-state UV/vis spectra; $^{e)}$Quantum yield is absolute quantum value measured by using an integrating sphere, polymer concentration: 1 mg/L.

effectively dissembles **P1** aggregates. Considering the fact that **P1** is a negatively charged CPE, cationic surfactants should be more effective than nonionic and anionic surfactants. Note that
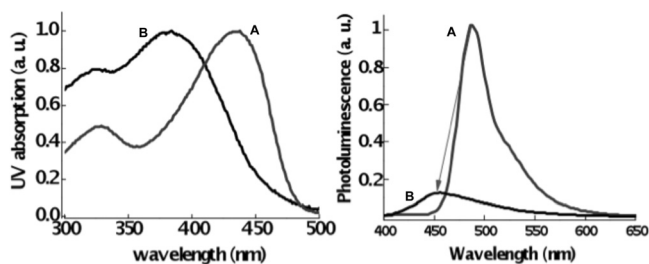
Figure 2. UV and Photoluminescence spectra of **P1** before (A, in chloroform) and after (B, in water) the cleavage of the ethylhexyl protecting group (**P1** conc. = 5 mgl^{-1}).
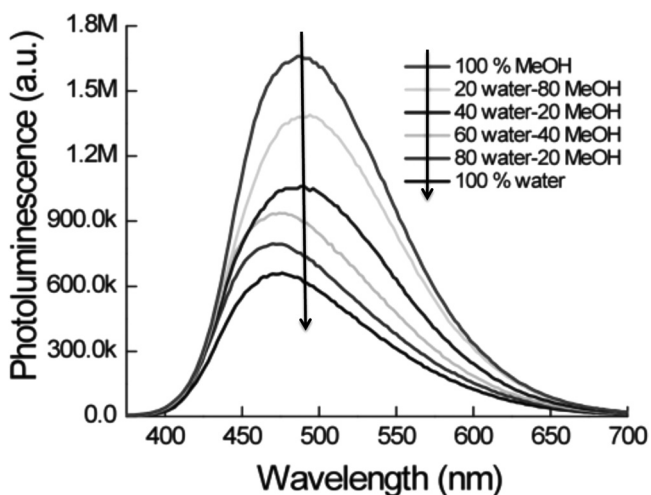
Figure 3. Photoluminescence spectra of **P1** in various water/methanol mixture solvents (**P1** conc. = 0.7 mgml^{-1}, excitation wavelength: 365 nm).

the increase in the fluorescence intensity of **P1** with increasing concentration of added DTAB was most significant between 0.1 wt% of DTAB and 0.5 wt% of DTAB. Interestingly, our calculation showed that 0.4 wt% of DTAB is required to make 1:1 charge complex with carboxylic acid groups of **P1** as schematically illustrated in **Figure 5**.[69] Distinct 0–0 and 0–1 emission bands are observed in Figure 4(c) indicating that DTAB effectively dissembles the **P1** aggregates.[48,53]

We investigated CPE aggregation in an aqueous environment by means of various electron microscopic techniques.[70–74] Conventional TEM microscopy images of **P1** shown in **Figure 6**a revealed tree-like, fractal aggregation suggesting that **P1** was completely aggregated. The magnified transition region shows that rigid rod-like **P1** chains aggregated to form cylindrical aggregates. A few single **P1** chains could aggregate into a fibril by hydrophobic π–π stacking and several fibrils could agglomerate to form few tens of nanometers wide fibers. However, this aggregated feature might be developed during the drying process for the conventional TEM sample preparation rather than representing the packing of **P1** in water. Therefore, we additionally conducted cryogenic TEM to observe an actual morphology of **P1** in aqueous environment. A **P1** solution in water was rapidly quenched in liquid ethane using cryo-plunge and images were obtained as a vitrified state below −170 °C. Interestingly, we observed a self-assembled sheet-like structure of **P1** from the cryo-images (Figure 6b). Hydrophobic interaction between the rigid-rod polymer chains likely induces the molecular packing and thin layer formation, followed by aggregation formation as schematically suggested in Figure 6c. We believed that the initially charged carboxylic acid group of **P1** was gradually protonated during the prolonged dialysis to remove oligomers and excess ions, accelerating the polymer aggregation as well. Therefore, even though **P1** was modified with water-soluble ionic and non-ionic side chains, **P1** molecules aggregate due to the rigidity and the hydrophobic nature of the main chain, resulting in the extremely low quantum yield of 0.45 in water.

**ADVANCED
FUNCTIONAL
MATERIALS**

www.afm-journal.de

www.MaterialsViews.com

*Materials
Views*
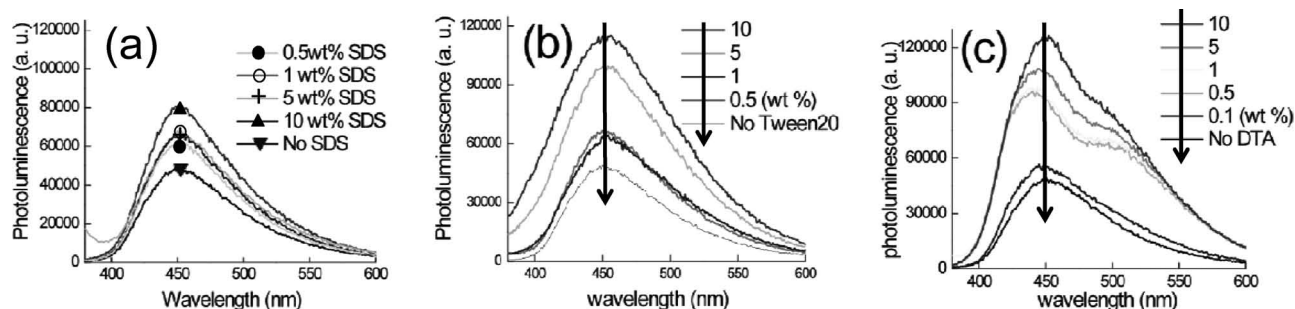
Figure 4. Photoluminescence profile of **P1** in water by adding different types of surfactants; a) SDS, negative, b) tween20, neutral, c) DTAB, positive (**P1** conc. = 5 mgml^{-1}).

2.4. P2: Preventing Aggregation by the Bulky Bifurcated Ethylene Oxide Side Chains

We replaced the single strand ethylene oxide side chains of **P1** with the bulky bifurcated ethylene oxide chain and prepared **P2** to efficiently sheath the rigid hydrophobic CPE backbone and minimize the π–π stacking (Figure 1).[53,60] Initially, we measured the molecular weight of **P2** by DMF-based GPC after the cleavage of the carboxy-protecting group. However, the molecular weight of **P2** was measured up to a few millions (gmol^{-1}) likely due to an incorrectly exaggerated hydrodynamic volume of the polymer caused by the limited solubility and aggregation of **P2** in DMF. The molecular weight of **P2** before the cleavage of the protection group measured by GPC was 32,100. The absorption and emission spectra of **P2** in water are presented in **Figure 7**. We examined the effect of the bulky ethylene oxide side chains in molecular aggregation by TEM and found that there was no large aggregation like the one found from **P1** even though **P2** solution was dried during the conventional TEM sample preparation. Instead, spherical particles of a few tens of nanometers in size were observed, suggesting that aggregation of CPE was efficiently suppressed by the bulky nonionic ethylene oxide side chains.[53,60] However, surprisingly even the non-aggregated **P2** in aqueous solution showed very low quantum yield of 0.9%

Figure 5. Schematic illustration of surfactant effect on **P1** in water.

while the **P2** derivative having the ethyl protected carboxylic acid side chains has 55.0% quantum yield in chloroform. Ionic-pendant groups having the sodium counter ions directly attached to the CPE backbone is hypothesized to be closely related with photoluminescence quenching of CPE in water. As supporting evidence, we found enhancement of emission intensity of **P1** and **P2** in an acidic condition where the carboxylic group should be protonated. It is believed that the observed quenching is attributed to the photoinduced electron transfer quenching mechanism as a result of the formation of electron donor/acceptor charge transfer complex between the polymer backbone and the directly connected ionic side chain.[75,76]

2.5. P3 and P4: Spacer Between the CPE Backbone and the Ionic Moiety

We put an alkyl spacer between the CPE backbone and the ionic pendant groups and prepared **P3** to exam the hypothesis that the direct connection of the ionic pendant group to the CPE backbone causes the emission quenching. **Figure 8** illustrates the absorption and the emission spectra of **P3**. The emission spectrum of **P3** shows a well-defined 0–0 band at the λ_{max} of 463 nm. As we expected, the aqueous solution of **P3** has the quantum yield of 31.6% (1 mgL^{-1}) that is dramatically improved from the 0.9% of the aqueous solution of **P2**, strongly supporting that the directly attached carboxylic acid groups to **P2** backbone cause the quenching. We previously prepared similar PPEs having sulfonate ionic groups via a propyloxy linkage and bifurcated ethylene oxide side chains. The sulfonated version of **P3** had a high quantum efficiency of 0.53 showing a good agreement with **P3**.[11] Conventional TEM microscopy images of 1 wt% **P3** aqueous solution was essentially identical to that of **P2** showing spherical nanoparticles of a few tens of nanometer.

We increased the length of the alkyl spacer from propyl (C$_3$) to hexyl (C$_6$) and prepared **P4** to test whether a long hydrophobic spacer would cause aggregation of CPE. Accordingly the quantum yield of the aqueous solution of **P4** significantly dropped down to 5.3%. Dialysis purification of **P4** also indicated that the longer hexyl hydrophobic chain lowers the solubility of **P4** in water. Conventional TEM microscopy images (data not shown) show that **P4** having the hexyl spacers are more aggregated in water than **P3** due to the long hydrophobic

www.MaterialsViews.com

ADVANCED
FUNCTIONAL
MATERIALS
www.afm-journal.de
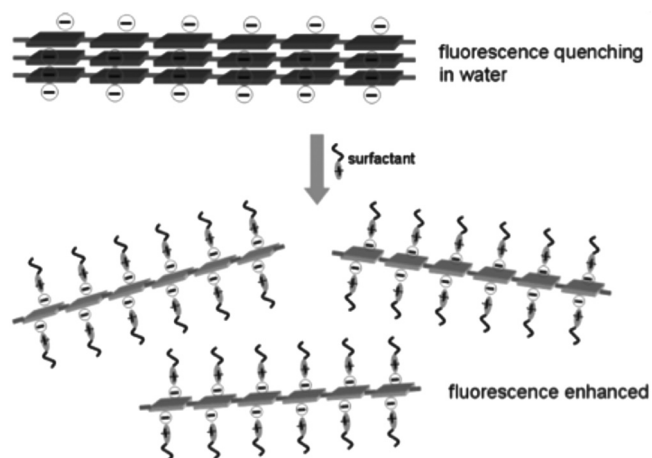
FULL PAPER
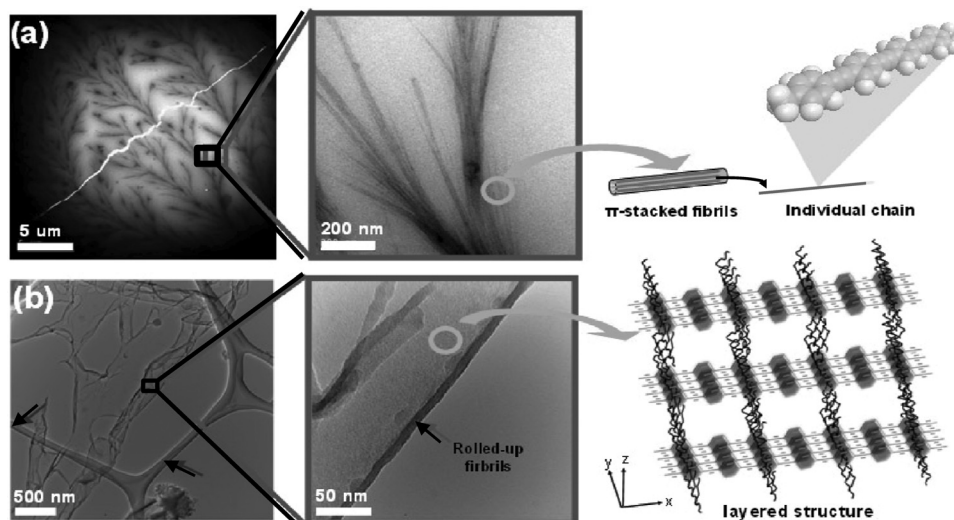
Figure 6. TEM microscopy images of **P1** in a) dried state and b) 1 w% water (arrows represent lacey carbons), c) proposed models for the aggregated structures of **P1** in air or water.
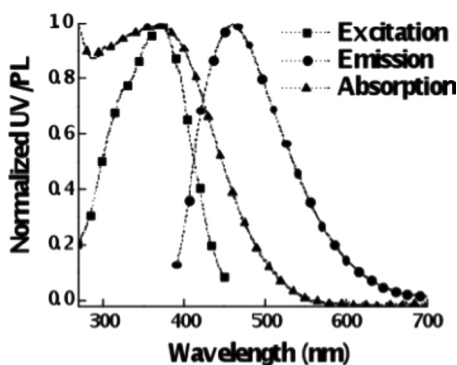
Figure 7. Absorption and Emission spectra of **P2** (10 mgL^{-1}) in water (excitation at 365 nm), excitation spectra of **P2** was obtained corresponding to the emission at 460 nm.
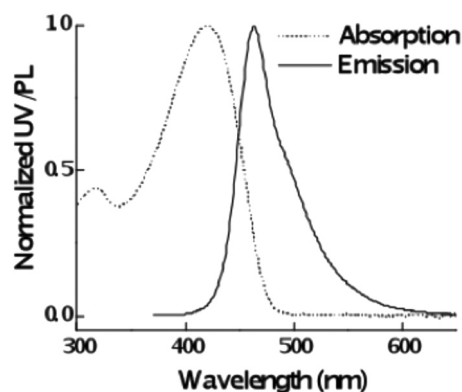
Figure 8. Normalized absorption (dotted) and emission (solid) spectra of **P3** (7 mgL^{-1}) in water (excitation at 365 nm).

alkyl spacers.[77–84] We hardly observed any significant aggregation during the dialysis of **P1**, **P2** and **P3** in water. Under visual observation, they remained soluble in deionized water and the solubility exceeded approximately 1 mg mL^{-1}. However, protonation of carboxylic group of **P4** during the dialysis induced precipitation of **P4**, indicating that the long alkyl spacers reduced the water-solubility of **P4** compared to other CPEs. After producing negative charges to **P4** in phosphate buffer (pH = 8) or in a slightly basic aqueous solution, the solubility of **P4** in water was significantly enhanced.

2.5. P5: Bulky Anionic Side Chain and Water-Soluble Spacer for the Ionic Side Chain

We replaced the hydrophobic alkyl linker with a hydrophilic ethylene oxide linker when we synthesized **P5** to prevent aggregation of CPE induced by the hydrophobic nature of the alkyl linker unit. **P5** completely dissolved in pure water (>10 mg/mL) and its solubility was independent to pH of the aqueous solution. **P5** was also soluble in a polar solvent such as dimethyl sulfoxide and methanol and partially soluble in tetrahydrofuran. Photoluminescence spectrum of **P5** in **Figure 9**(a) is narrow with a well-defined 0–0 band at 457 nm. **P5** has the highest fluorescent emission quantum yield of 51.4% (1 mgL^{-1}) among other CPEs and is over 110 times more emissive than **P1**.
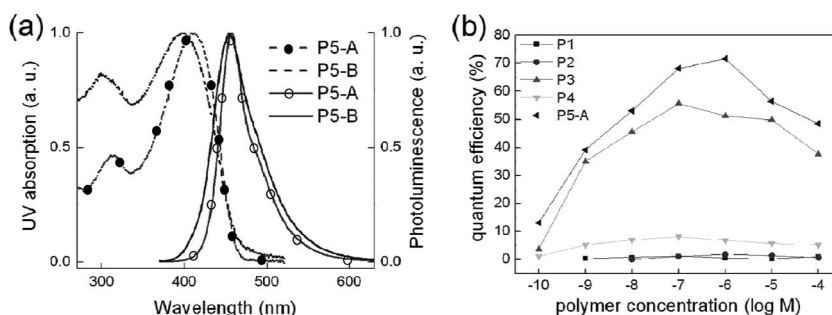
Figure 9. a) UV and PL spectra (5 mgL^{-1}) of **P5** and **P5-A** (Polymers were excited at 365 nm), b) fluorescence quantum yield of all polymers (**P1** to **P5**) at various concentrations.

FULL PAPER
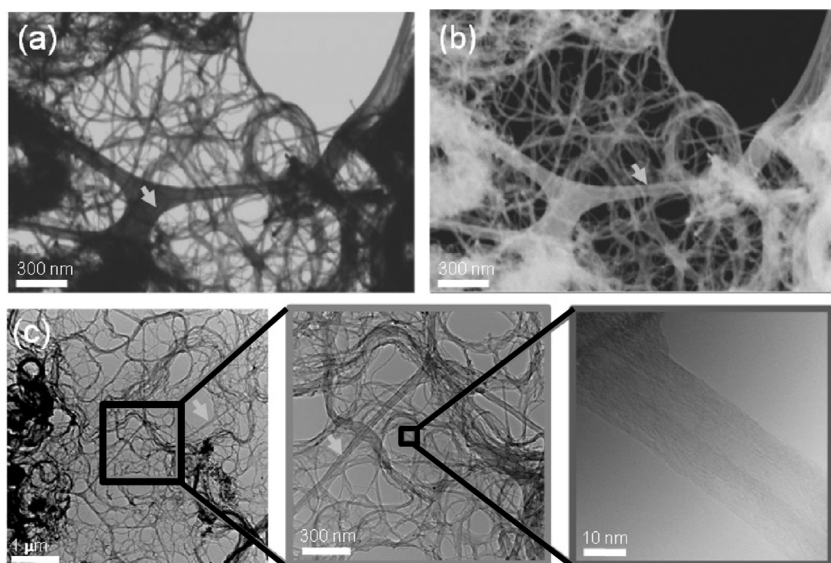
Figure 10. Electron microscopy images of **P5**; a) SEM (SE2 mode, 30 kV) and b) transmission mode (STEM) and c) conventional TEM images (200 kV). All samples were prepared with 1 wt% solution in water on a lacey carbon film (indicated by the arrows in the figures) and dried in air.

Electron microscopic analysis for **P5** did not show any significant aggregation, indicating that the hydrophilic nature of the side chain is necessary to prevent CPE aggregation in water. As shown using the scanning transmission electron microscope (STEM) and the conventional TEM (**Figure 10**), agglomeration of **P5** was noticeably suppressed while **P1** or **P4** showed a micrometer-sized massive aggregation. From the conventional TEM images one can apparently observe fibrils of approximately 25 nm (Figure 10c). Molecular mechanics calculations carried out using MM2 force field predicted that a hydrophobic backbone of **P5** would be wrapped by the hydrophillic side chains and the resulting thickness of the polymer chain would be 2.4 nm. Therefore, the observed fibrils are likely composed of only a few of polymer chains even after water evaporated slowly during the TEM sample preparation. These results lead to a reasonable conclusion that hardly any π–π stacking among **P5** forms in water. We also additionally carried out cryogenic TEM of **P5** in aqueous environment to further investigate the correlation between the nature of the side chain and the aggregation behavior of CPE. A spider web-like entangled structure formed by the rigid rod-like **P5** chains shown in **Figure 11** clearly indicates discrete polymer chains without agglomeration throughout the whole area. The thickness of the polymer chain in the cyro-TEM image is about 7 nm, that is, thicker than 2.4 nm predicted by molecular modeling. The clumps found along the polymer chain in the middle figure are ice crystals formed during the cryo-TEM sample preparation. The cryo-TEM analysis convincingly reveals the non-aggregated morphology of **P5** in water.

We additionally investigated the concentration dependence of the quantum yield of the CPEs. As shown in Figure 9b, the quantum yield of CPEs in water has the same trend of other fluorophores in organic solvents. They mostly show the highest fluorescence efficiency at submicromolar concentration regime

and as the concentration increased above that regime the quantum yield decreased showing the concentration dependent self-quenching.

Finally, we prepared **P5-A** which has two directly-attached carboxylic acid units at the chain ends to investigate further the influence of carboxylic acid group to the emissive property of CPEs. In situ end-capping reaction to **P5** during polymerization was undertaken by adding 4-ethynyl-benzoic acid with additional palladium catalyst (**Scheme 3**).[11,85–87] As shown in Figure 9a, the chain end modification essentially did not cause any spectral broadening nor bathochromic shift, indicating minimal influence on the solubility of **P5-A** and negligible aggregation of **P5-A** in water. **P5-A** indeed showed a similar solubility in water and identical TEM images as **P5**. However, the quantum yield of **P5-A** was largely reduced to 31.6% that is 38.5% drop from 51.4% of **P5**, clearly demonstrating that a directly-connected ionic group to the conjugated backbone of CPEs has a detrimental effect to the emission property of CPEs.[88]

3. Conclusion

We systematically investigated the effect of the chemical nature, shape, and the length of the ionic and nonionic side chains on the water solubility and quantum yield of conjugated polyelectrolytes by means of electron microscopy and spectroscopic analysis. Simple ionic and anionic decoration of CPE did not warrant good water-solubility because of the rigid and hydrophobic nature of the conjugated backbone of CPEs. TEM analysis combined with quantum yield measurement reveals that unless CPEs are modified with bulky hydrophilic ethylene oxide side chains, CPEs form aggregates in water and consequent fluorescence quenching. Carboxylic acid group, which is a commonly used and convenient functional group for
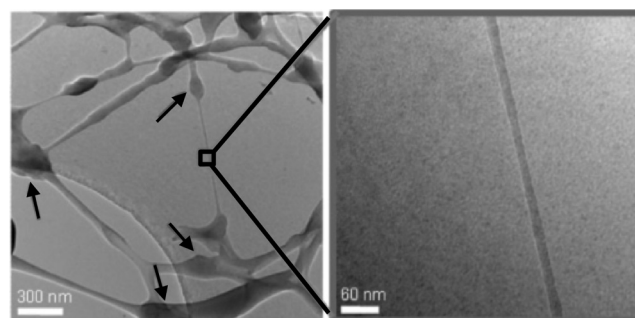
Figure 11. Cryo-TEM images of **P5-A** (1 wt% in water, applied voltage: 120 kV). The sample was prepared with 1 wt% solution in water on a formvar-coated grid, stabilized with evaporated carbon film. Massive lumps (arrows) in the left figure are ice crystals.

www.MaterialsViews.com

**ADVANCED
FUNCTIONAL
MATERIALS**
www.afm-journal.de

FULL PAPER
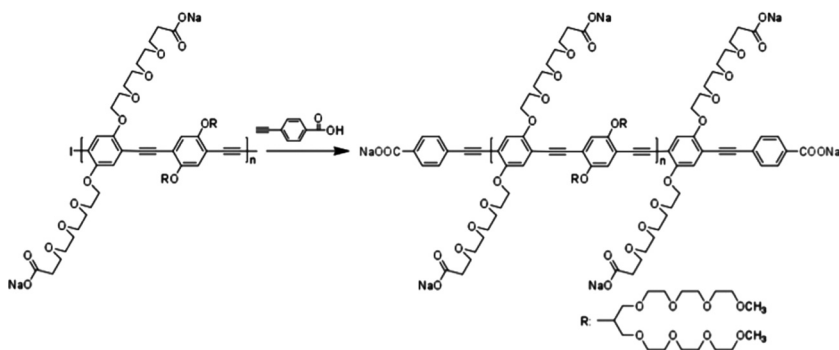
Scheme 3. In situ end-capping reaction for **P5-A**.

to enhance contrast. Sample preparation for Figure 10 was done in a similar way and SEM and TEM images were respectively obtained using Ultra55 Field Emission Scanning Electron Microscope (FESEM, Zeiss, 30 kV) and JEOL 2100 TEM (acceleration voltage: 200 kV). For cryo-TEM images, a carbon coated film on a broken pattern consists of woven-mesh-like holes (300 mesh) or a formvar coated grid, stabilized with evaporated carbon film were purchased from Electron Microscopy Sciences, Inc (PA, USA) and a cryoplunge (Gatan, Inc, CA, USA) was used for polymer sample preparation. The specimen grid was clamped between the tips of plunging tweezers and 3 μL of polymer solution (1 w% or 0.1 wt% in water) was blotted to grid for production of thin, aqueous film. It is then plunged into a temperature controlled ethane bath (<–170 °C) and polymer solution is rapidly frozen as vitrified ice. Sample was stored in liquid nitrogen until use. The grid was transferred to the TEM for unstained, in situ observation. Images were taken in the bright-field mode with JEOL 2100 transmission electron microscope at 120 kV accelerating voltage.

bioconjugation, turned out to have a detrimental influence on the emissive property of CPE when it is connected directly to the CPE backbone. Placing a spacer linker between carboxylic acid and the CPE backbone solved the quenching problem. However, the nature and the length of the spacer group also largely influence on the water-solubility of CPEs. When the alkyl linker was long, the hydrophobic nature of the linker induced self-assembled aggregates. The presented results reveal the effects of the side chain design on the water-solubility and the consequent emissive property of CPEs and provide a molecular design principle to achieve highly emissive, completely water-soluble, and conveniently functionalized CPEs.

4. Experimental Section

Materials and Methods: All chemicals were purchased from Sigma-Aldrich, Inc. or Acros Organics, Inc. and used without further purification. Compounds **1**,[89,90] **2**,[91,92] **M5**[50] and **M6**[50,60,93] in Schemes 1 and 2 are prepared according to the literature published previously. All polymers (**P1** to **P5** and **P5-A**) were purified by dialysis against deionized water (molecular weight cut-off: 12,000–14,000 gmol⁻¹) for 3 days, lyophilized to dry the polymer, and stored in the dried state at 4 °C. The molecular weight of all CPEs except **P5** was determined by GPC with the polystyrene references in THF before the cleavage of the ethylhexyl protecting group of carboxylic acid. Due to the limited solubility of **P5** in THF, its number-averaged molecular weight (M_n) was calculated by ^{1}H NMR end-group analysis. NMR characterization was done with Varian Inova 500 (500 MHz, 11.7 T, Tin)

Photophysical Experiments: UV/vis absorption spectra of the CPE solutions were obtained on a Cary UV50 UV/Vis spectrometer (Varian, Inc.). Steady-state fluorescence spectra of the CPEs were recorded on a PTI QuantaMaster spectrofluorometer™. The molar concentration of the CPE solutions was determined based on the repeat unit of the CPEs. Corrected fluorescence spectra were obtained for variations in photomultiplier response over wavelength using correction curves generated on the instrument. The fluorescence spectra were normalized by the optical density corresponding to the highest fluorescence intensity. The quantum yields of the CPEs in various concentrations were measured by exciting the CPEs at 365 nm in deionized water using an integrating sphere attached to the PTI QuantaMaster spectrofluorometer.

Electron Microscopy Analysis: A copper TEM grid coated with a 20–30 nm film of pure carbon (purchased from Electron Microscopy Sciences, PA, USA) was held at the tip of a tweezer. A small drop of aqueous CPE solution was placed on the grid to form a bead. An excess samples in water were blotted off by touching the grid with a filter paper and the sample was left for drying. Images were taken in the bright-field mode with a Tecnai G2 12 Twin transmission electron microscope at 120 kV accelerating voltage. Structures were imaged at slight underfocus in order

[1] M. Pinto, K. S. Schanze, *Synthesis* **2002**, *9*, 1293–1309.
[2] H. Jiang, P. Taranekar, J. R. Reynolds, K. S. Schanze, *Angew. Chem. Int. Ed.* **2009**, *48*, 4300–4316.
[3] F. Feng, H. Wang, L. Han, S. Wang, *J. Am. Chem. Soc.* **2008**, *130*, 11338–11343.
[4] H. Li, R. Yang, G. C. Bazan, *Macromolecules* **2008**, *41*, 1531–1536.
[5] M. Kang, O. K. Nag, R. R. Nayak, S. Hwang, H. Suh, H. Y. Woo, *Macromolecules* **2009**, *42*, 2708–2714.
[6] G. C. Bazan, S. Wang, L. Liu, L. An, *Angew, Chem. Int. Ed.* **2009**, *48*, 4372–4375.
[7] H.-A. Ho, M. Béra-Abérem, M. Leclerc, *Chem. Eur. J.* **2005**, *11*, 1718–1724 and references therein.
[8] K. P. R. Nilsson, O. Inganäs, *Nat. Mater.* **2003**, *2*, 419–424.
[9] B. Liu, G. C. Bazan, *Chem. Mater.* **2004**, *16*, 4467–4476 and references therein.
[10] C. J. Yang, M. Pinto, K. Schanze, W. Tan, *Angew. Chem. Int. Ed.* **2005**, *44*, 2572–2576.
[11] K. Lee, L. K. Povlich, J. Kim, *Adv. Funct. Mater.* **2007**, *17*, 2580–2587.
[12] B. Liu, G. C. Bazan, *Proc. Natl. Acad. Sci. USA.* **2005**, *102*, 589–593.
[13] K. Lee, J.-M. Rouillard, T. Pham, E. Gulari, J. Kim, *Angew. Chem. Int. Ed.* **2007**, *46*, 4667–4670.
[14] C.-C. Pun, K. Lee, H.-J. Kim, J. Kim, *Macromolecules.* **2006**, *39*, 7461.
[15] M. B. Abérem, A. Najari, H.-A. Ho, J.-F. Gravel, P. Nobert, D. Boudreau, M. Leclerc, *Adv. Mater.* **2006**, *18*, 2703–2707.
[16] D. Yu, Y. Zhang, B. Liu, *Macromolecules* **2008**, *41*, 4003–4011.
[17] K.-Y. Pu, B. Liu, *Macromolecules* **2008**, *41*, 6636–6640.
[18] F. Feng, Y. Tang, S. Wang, Y. Li, D. Zhu, *Angew. Chem. Int. Ed.* **2007**, *46*, 7882–7886.
[19] C. Fan, K. W. Plaxco, A. J. Heeger, *J. Am. Chem. Soc.* **2002**, *124*, 5642–5643.
[20] L. Chen, D. W. McBranch, H.-L. Wang, R. Helgeson, F. Wudl, D. G. Whitten, *Proc. Natl. Acad. Sci. USA.* **1999**, *96*, 12287–12292.
[21] K. P. R. Nilsson, A. Herland, P. Hammerström, O. Inganäs, *Biochemistry* **2005**, *44*, 3718–3724.

[22] X. Song, H. Wang, J. Shi, J.-W. Park, B. I. Swanson, *Chem. Mater.* **2002**, *14*, 2342–2347.

[23] I.-B. Kim, A. Dunkhorst, U. H. F. Bunz, *Langmuir* **2005**, *21*, 7985–7989.

[24] S. J. Dwight, B. S. Gaylord, J. W. Hong, G. C. Bazan, *J. Am. Chem. Soc.* **2004**, *126*, 16850–16859.

[25] P. Björk, A. Herland, I. G. Scheblykin, O. Inganäs, *Nano Lett.* **2005**, *5*, 1948–1953.

[26] R. L. McRae, R. L. Phillips, I. B. Kim, U. H. F. Bunz, C. J. Fahrni, *J. Am Chem. Soc.* **2008**, *130*, 7851–7853.

[27] J. H. Moon, W. McDaniel, P. MacLean, L. E. Hancock, *Angew, Chem. Int. Ed.* **2007**, *46*, 8223–8225.

[28] K.-Y. Pu, B. Liu, *Adv. Funct. Mater.* **2011**, *21*, 3408–3423.

[29] J. S. Wilson, M. J. Frampton, J. J. Michels, L. Sardone, G. Marletta, R. H. Friend, P. Samorí, H. L. Anderson, F. Cacialli, *Adv. Mater.* **2005**, *17*, 2659–2663.

[30] J. H. Seo, T.-Q. Nguyen, *J. Am. Chem. Soc.* **2008**, *130*, 10042–10043.

[31] J. M. Hodgkiss, G. Tu, S. Albert-Seifried, W. T. S. Huck, R. H. Friend, *J. Am. Chem. Soc.* **2009**, *131*, 8913–8921.

[32] W. Ma, P. K. Iyer, X. Gong, B. Liu, D. Moses, G. C. Bazan, A. J. Heeger, *Adv. Mater.* **2005**, *17*, 274–277.

[33] R. Yang, H. Wu, Y. Cao, G. C. Bazan, *J. Am. Chem. Soc.* **2006**, *128*, 14422–14423.

[34] E. Smela, *Adv. Mater.* **2003**, *15*, 481–494.

[35] T. M. Swager, *Acc. Chem. Res.* **1998**, *31*, 201–207.

[36] D. T. McQuade, A. E. Pullen, T. M. Swager, *Chem. Rev.* **2000**, *100*, 2537–2574.

[37] C. Tan, E. Atas, J. G. Müller, M. R. Pinto, V. D. Kleiman, K. S. Schanze, *J. Am. Chem. Soc.* **2004**, *126*, 13685–13694.

[38] B. S. Harrison, M. B. Ramey, J. R. Reynolds, K. S. Schanze, *J. Am. Chem. Soc.* **2000**, *122*, 8561–8562.

[39] S. A. Kushon, K. D. Ley, K. Bradford, R. M. Jones, D. McBranch, D. Whitten, *Langmuir* **2002**, *18*, 7245.

[40] C. Tan, M. R. Pinto, K. S. Schanze, *Chem. Commun.* **2002**, 446–447.

[41] G. D. Joly, L. Geiger, S. E. Kooi, T. M. Swager, *Macromolecules* **2006**, *39*, 7175–7177.

[42] M. R. Pinto, B. M. Kristal, K. S. Schanze, *Langmuir* **2003**, *19*, 6523–6533.

[43] H. Jiang, X. Zhao, K. S. Schanze, *Langmuir* **2006**, *22*, 5541–5543.

[44] X. Zhao, H. Hui, K. S. Schanze, *Macromolecules* **2008**, *41*, 3422–3428.

[45] K. Lee, L. Povlich, J. Kim, *Analyst* **2010**, *135*, 2179–2189.

[46] F. Wang, G. C. Bazan, *J. Am. Chem. Soc.* **2006**, *128*, 15786–15792.

[47] S. A. Jenekhe, J. A. Osaheni, *Science* **1994**, *265*, 765–768.

[48] J. Kim, T. M. Swager, *Nature* **2001**, *411*, 1030–1034.

[49] Y. Q. Wang, A. J. Zappas, J. N. Wilson, I.-B. Kim, K. M. Solntsev, L. M. Tolbert, U. H. F. Bunz, *Macromolecules* **2008**, *41*, 1112–1117.

[50] I. B. Kim, R. Phillips, U. H. F. Bunz, *Macrmolecules* **2007**, *40*, 5290–5293.

[51] Y. Wang, A. J. Zappas II, J. N. Wilson, I.-B. Kim, K. M. Solntsev, L. M. Tolbert, U. H. F. Bunz, *Macromolecules* **2008**, *41*, 1112–1117.

[52] J. H. Wosnick, C. M. Mello, T. M. Swager, *J. Am. Chem. Soc.* **2005**, *127*, 3400–3405.

[53] K. Lee, J. C. Cho, J. Deheck, J. Kim, *Chem. Commun.* **2006**, 1983–1985.

[54] H.-A. Ho, M. Leclerc, *J. Am. Chem. Soc.* **2004**, *126*, 1384–1387.

[55] K. Doré, S. Dubus, H.-A. Ho, I. Lévesque, M. Brunette, G. Corbeil, M. Boissinot, G. Boivin, M. G. Bergeron, D. Doudreau, M. Leclerc, *J. Am. Chem. Soc.* **2004**, *126*, 4240–4244.

[56] H. A. Ho, K. Doré, M. Boissinot, M. G. Bergeron, R. M. Tanguay, D. Bourdreau, M. Leclerc, *J. Am. Chem. Soc.* **2005**, *127*, 12673–12676.

[57] H.-A. Ho, M. Boissinot, M. G. Bergeron, G. Corbeil, K. Doré, D. Bourdreau, M. Leclerc, *Angew. Chem. Int. Ed.* **2002**, *41*, 1548–1551.

[58] I. B. Kim, R. Phillips, U. H. F. Bunz, *Macromolecules* **2007**, *40*, 5290–5293.

[59] R. L. Phillips, O. R. Miranda, C.-C. You, V. M. Rotello, U. H. F. Bunz, *Angew. Chem. Int. Ed.* **2008**, *47*, 2590–2594.

[60] A. Khan, S. Müller, S. Hecht, *Chem. Commun.* **2005**, 584–586.

[61] H.-Y. Liao, C.-H. Cheng, *J. Org. Chem.* **1995**, *60*, 3711–3716.

[62] V. Subramanian, V. R. Batchu, D. Barange, M. Pal, *J. Org. Chem.* **2005**, *70*, 4778–4783.

[63] C. Lambert, K. Utimoto, H. Nozaki, *Tetrahedron Lett.* **1984**, *25*, 5323–5326.

[64] A. F. Thünemann, *Adv. Mater* **1999**, *11*, 127.

[65] J. J. Lavigne, D. L. Broughton, J. N. Wilson, B. Erdogan, U. H. F. Bunz, *Macromolecules* **2003**, *36*, 7409–7412.

[66] L. Chen, S. Xu, D. McBranch, D. Whitten, *J. Am. Chem. Soc.* **2000**, *122*, 9302–9303.

[67] A. F. Thünemann, D. Ruppelt, *Langmuir* **2001**, *17*, 5098–5102.

[68] H. D. Burrows, V. M. M. Lobo, J. Pina, M. L. Ramos, J. Seixas de Melo, A. J. M. Valente, M. J. Tapia, S. Pradhan, U. Scherf, *Macromolecules* **2004**, *37*, 7425–7427.

[69] This value is calculated based on the molecular weight of polymer repeat unit (658.60 g/mol).

[70] Y. Talmon, *Ber. Bunsenges. Phys. Chem.* **1996**, *100*, 364–372.

[71] D. Danino, A. Bernheim-Groswasser, Y. Talmon, *Colloids Surf. A* **2001**, *183–185*, 113.

[72] Z. Li, E. Kesselman, Y. Talmon, M. A. Hillmyer, T. P. Lodge, *Science* **2004**, *306*, 98–101.

[73] D. J. Pochan, L. Pakstis, B. Ozbas, A. P. Nowak, T. J. Deming, *Macromolecules* **2002**, *35*, 5358–5360.

[74] M. S. Lamm, K. Rajagopal, J. P. Schneider, D. J. Pochan, *J. Am. Chem. Soc.* **2005**, *127*, 16692–16700.

[75] B. Xie, M. Bagui, R. Guo, K. Li, Q. Wang, Z. Peng, *J. Poly. Sci. Part A: Polym. Chem.* **2007**, *45*, 5123–5135.

[76] C. B. Murphy, Y. Zhang, T. Troxler, V. Ferry, J. J. Martin, W. E. Jones Jr., *J. Phys. Chem. B* **2004**, *108*, 1537–1543.

[77] There is research on π–π aggregation induced self-assembly of conjugated oligomer/polymers: C. Tan, M. R. Pinto, M. E. Kose, I. Ghiviriga, K. S. Schanze, *Adv. Mater.* **2004**, *16*, 1208–1211.

[78] J. S. Moore, *Acc. Chem. Res.* **1997**, *30*, 402–413.

[79] J. C. Nelson, J. G. Saven, J. S. Moore, P. G. Wolynes, *Science* **1997**, *277*, 1793–1796.

[80] L. Brunsveld, B. J. B. Folmer, E. W. Meijer, *Chem. Rev.* **2001**, *101*, 4071–4097.

[81] L. M. Herz, C. Daniel, C. Silva, F. J. M. Hoeben, A. P. H. J. Schenning, E. W. Meijer, R. H. Friend, R. T. Phillips, *Phys. Rev. B* **2003**, *68*, 045203.

[82] J. N. Wilson, W. Steffen, T. G. McKenzie, G. Lieser, M. Oda, D. Neher, U. H. F. Bunz, *J. Am. Chem. Soc.* **2002**, *124*, 6830–6831.

[83] W. Steffen, B. Köhler, M. Altmann, U. Scherf, K. Stitzer, U. H. F. Loye, H.-C. Z. Bunz, *Chem. Eur. J.* **2001**, *7*, 117.

[84] U. H. F. Bunz, V. Enkelmann, L. Kloppenburg, D. Jones, K. D. Shimizu, J. B. Claridge, H.-C. Z. Loye, G. Lieser, *Chem. Mater.* **1999**, *11*, 1416.

[85] P. Samorí, N. Severin, K. Müllen, J. P. Rabe, *Adv. Mater.* **2000**, *12*, 579.

[86] V. Samorí P.Francke, K. Müllen, J. P. Rabe, *Chem. Eur. J.* **1999**, *5*, 2312–2317.

[87] K. Kuroda, T. M. Swager, *Macromolecules* **2004**, *37*, 716–724.

[88] Even though we consistently observed fluorescence intensity drop caused by the directly attached carboxylic acid group through various conjugated polyelectrolytes, oligomers with directly attached carboxylic acids having a large quantum yield were also reported: C. A. Stanier, M. J. O'Connell, W. Clegg, H. L. Anderson, *Chem. Commun.* **2001**, 493.

[89] H. Häger, W. Heitz, *Macromol. Chem. Phys.* **1998**, *199*, 1821–1826.

[90] R. J. Perry, B. D. Wilson, S. R. Turner, R. W. Blevins, *Macromolecules* **1995**, *28*, 3509–3515.

[91] J. Zhang, Y. Cui, M. Wang, Liu, *J. Chem. Commun.* **2002**, 2526–2527.

[92] Q. Zhou, T. M. Swager, *J. Am. Chem. Soc.* **1995**, *117*, 12593–12602.

[93] U. Lauter, W. H. Meyer, V. Enkelmann, G. Wegner, *Macromol. Chem. Phys.* **1998**, *199*, 2129–2140.